Appendix 11F Smelt Analysis

Appendix 11F Smelt Analysis

11F.1 Introduction

This appendix describes quantitative methods and supplementary results used in the impact analyses of delta smelt and longfin smelt: the *Eurytemora affinis*–X2 analysis for smelt prey, upstream sediment entrainment, the Sacramento–San Joaquin Delta (Delta) outflow–longfin smelt abundance analysis, the Delta outflow–longfin smelt abundance analysis (based on Nobriga and Rosenfield 2016), the X2–longfin smelt abundance index analysis, and tidal habitat restoration mitigation calculations for longfin smelt.

11F.2 *Eurytemora affinis*–X2 Analysis

This analysis followed Kimmerer's (2002) methods to conduct an analysis of the relationship between the smelt zooplankton prey *Eurytemora affinis* and spring (March–May) X2 for the period from 1980 to 2017, as described by Greenwood (2018). The main steps in preparing the data for analysis were as follows:

1. Historical zooplankton data were obtained from California Department of Fish and Wildlife (2018).
    a. Data were subset to only include surveys 3, 4, and 5 (March–May).
    b. Specific conductance was converted to salinity by applying Schemel's (2001) method, then only samples within the low salinity zone (salinity = 0.5–6) were selected.
    c. A constant of 10 was added to *E. affinis* adult catch per unit effort (number per cubic meter) in each sample, then the resulting value was $\log_{10}$-transformed.
    d. The $\log_{10}$-transformed values were averaged first by month, and then by year.
2. Historical X2 data were obtained from DAYFLOW (https://www.water.ca.gov/Programs/Environmental-Services/Compliance-Monitoring-And-Assessment/Dayflow-Data).
    a. For years prior to water year 1997 (which is the year DAYFLOW X2 values began to be provided), the DAYFLOW daily predictive equation for X2 was used, based on a starting value from Anke Mueller-Solger (see Greenwood 2018 for details).
    b. The mean March–May X2 was calculated for each year.

Similar to Kimmerer (2002), a generalized linear model (GLM) was used to regress mean annual $\log_{10}$-transformed *E. affinis* catch per unit effort against mean March–May X2, including a step change between 1987 and 1988 to reflect the *Potamocorbula amurensis* clam invasion and a step change between 2002 and 2003 to reflect the onset of the Pelagic Organism Decline (POD; Thomson et al. 2010). The interaction of X2 and the step change was included in a full model, but the interaction was not statistically significant, so the model was rerun with only X2 and the step changes included. These analyses were conducted in SAS 9.4 software.[1] The statistical outputs indicate that there is little difference in the regression coefficients for the post-*Potamocorbula* and POD step changes, whereas both regression coefficients were significantly less than the coefficient for the pre-*Potamocorbula* period. Regression coefficients from the model were stored for prediction of *E. affinis* relative abundance for the No Action Alternative (NAA)[2] and Alternative 1–3 scenarios.

The stored regression coefficients from the regression of historical *E. affinis* catch per unit effort vs. X2 and step changes were then applied to the NAA and Alternative 1–3 scenarios using PROC PLM in SAS 9.4 software. The basic regression model being applied was:

$$\log_{10}(\textit{E. affinis}\text{ catch per unit effort}) = 3.9404 – 0.0152\ (\text{mean March–May X2}) – 0.7863$$

where 3.9404 is the intercept and -0.7863 is the coefficient for the POD step change (the POD step change being chosen because it represents the most recent time period). Predictions were back-transformed to the original measurement scale (catch per unit effort, number per cubic meter) for summary of results. X2 inputs for the analysis came from the DSM2 modeling of water years 1922–2003 for the NAA and Alternative 1–3 scenarios.

Results of the analysis are summarized in the main body of Chapter 11, *Aquatic Biological Resources*. Tables 11F-1 through 11F-5 provide supplemental information also discussed in the main body of Chapter 11.

Table 11F-1. *Eurytemora affinis*–X2 Analysis: Mean and 95% Prediction Limits, NAA

Year	Mean Estimate	Lower 95% Prediction Limit	Upper 95% Prediction Limit
1922	176	25	967
1923	125	16	695
1924	68	5	410
1925	145	20	797
1926	127	16	706
1927	192	28	1,061
1928	159	22	878
1929	75	6	441

[1] Copyright 2002–2012, SAS Institute Inc. SAS and all other SAS Institute Inc. product or service names are registered trademarks or trademarks of SAS Institute Inc., Cary, NC, USA

[2] The term *NAA*, which is identical to the No Project Alternative, is used throughout Chapter 11, *Aquatic Biological Resources*, and associated aquatic resources appendices in the presentation of modeled results and represents no material difference from the No Project Alternative, as discussed in Chapter 3, *Environmental Analysis*.

Year	Mean Estimate	Lower 95% Prediction Limit	Upper 95% Prediction Limit
1930	115	14	644
1931	64	4	389
1932	99	11	563
1933	79	7	460
1934	83	8	483
1935	163	23	900
1936	158	22	868
1937	171	24	940
1938	205	30	1,134
1939	77	6	453
1940	184	27	1,012
1941	204	30	1,132
1942	189	28	1,041
1943	175	25	966
1944	105	12	589
1945	134	18	739
1946	116	14	646
1947	100	11	566
1948	132	17	731
1949	132	17	730
1950	133	17	735
1951	146	20	802
1952	205	30	1,134
1953	138	18	760
1954	173	25	955
1955	77	6	452
1956	183	27	1,011
1957	151	21	834
1958	205	30	1,133
1959	99	11	562
1960	108	13	605
1961	100	11	565
1962	124	16	691
1963	184	27	1,013
1964	74	6	437
1965	162	23	893

Year	Mean Estimate	Lower 95% Prediction Limit	Upper 95% Prediction Limit
1966	122	15	676
1967	205	30	1,133
1968	118	15	660
1969	205	30	1,134
1970	132	17	728
1971	174	25	957
1972	121	15	672
1973	160	22	882
1974	188	27	1,037
1975	183	27	1,011
1976	70	5	417
1977	61	3	377
1978	189	28	1,041
1979	149	20	821
1980	162	23	893
1981	115	14	644
1982	204	30	1,128
1983	205	30	1,134
1984	146	20	807
1985	95	10	538
1986	164	23	905
1987	101	11	573
1988	74	6	439
1989	143	19	791
1990	72	5	427
1991	104	12	587
1992	101	11	573
1993	197	29	1,090
1994	75	6	442
1995	205	30	1,134
1996	205	30	1,134
1997	136	18	754
1998	205	30	1,134
1999	175	25	963
2000	165	23	908
2001	111	13	620

Year	Mean Estimate	Lower 95% Prediction Limit	Upper 95% Prediction Limit
2002	116	14	646
2003	163	23	897

Table 11F-2. *Eurytemora affinis*–X2 Analysis: Mean and 95% Prediction Limits, Alternative 1A

Year	Mean Estimate	Lower 95% Prediction Limit	Upper 95% Prediction Limit
1922	175	25	965
1923	125	16	695
1924	69	5	412
1925	145	20	799
1926	127	16	705
1927	191	28	1,053
1928	159	22	877
1929	75	6	441
1930	114	14	638
1931	64	4	389
1932	99	11	563
1933	79	7	460
1934	83	8	480
1935	162	23	891
1936	158	22	868
1937	170	24	935
1938	205	30	1,134
1939	77	6	452
1940	183	27	1,011
1941	204	30	1,132
1942	189	28	1,041
1943	175	25	966
1944	105	12	589
1945	134	18	739
1946	116	14	646
1947	100	11	566
1948	132	17	732
1949	130	17	721
1950	133	17	734

Year	Mean Estimate	Lower 95% Prediction Limit	Upper 95% Prediction Limit
1951	145	20	801
1952	205	30	1,134
1953	138	18	760
1954	173	25	955
1955	77	6	452
1956	182	26	1,005
1957	149	20	823
1958	205	30	1,133
1959	99	11	562
1960	107	12	601
1961	99	11	562
1962	123	16	685
1963	183	27	1,010
1964	74	6	437
1965	161	23	889
1966	122	15	676
1967	205	30	1,133
1968	118	15	659
1969	205	30	1,134
1970	131	17	724
1971	174	25	957
1972	118	15	659
1973	160	22	882
1974	188	27	1,037
1975	183	27	1,011
1976	70	5	417
1977	61	3	376
1978	191	28	1,057
1979	148	20	817
1980	162	23	893
1981	114	14	635
1982	204	30	1,128
1983	205	30	1,134
1984	147	20	808
1985	94	10	538
1986	164	23	904

Year	Mean Estimate	Lower 95% Prediction Limit	Upper 95% Prediction Limit
1987	100	11	566
1988	74	6	438
1989	142	19	784
1990	72	5	427
1991	102	11	576
1992	101	11	571
1993	197	29	1,087
1994	74	6	440
1995	205	30	1,134
1996	205	30	1,134
1997	136	18	754
1998	205	30	1,134
1999	175	25	963
2000	165	23	908
2001	109	13	612
2002	116	14	645
2003	162	23	891

Table 11F-3. *Eurytemora affinis*–X2 Analysis: Mean and 95% Prediction Limits, Alternative 1B

Year	Mean Estimate	Lower 95% Prediction Limit	Upper 95% Prediction Limit
1922	175	25	965
1923	126	16	697
1924	69	5	412
1925	144	20	797
1926	127	16	706
1927	191	28	1,053
1928	159	22	877
1929	75	6	441
1930	114	14	638
1931	64	4	389
1932	99	11	563
1933	79	7	460
1934	83	8	480
1935	162	23	891

Year	Mean Estimate	Lower 95% Prediction Limit	Upper 95% Prediction Limit
1936	158	22	868
1937	170	24	935
1938	205	30	1,134
1939	76	6	448
1940	183	27	1,011
1941	204	30	1,132
1942	189	28	1,041
1943	175	25	966
1944	105	12	589
1945	134	18	739
1946	116	14	646
1947	100	11	566
1948	132	17	733
1949	130	17	721
1950	133	17	734
1951	145	20	801
1952	205	30	1,134
1953	138	18	760
1954	173	25	955
1955	77	6	452
1956	182	26	1,006
1957	150	21	824
1958	205	30	1,133
1959	99	11	562
1960	107	12	602
1961	99	11	563
1962	123	16	685
1963	183	27	1,010
1964	74	6	437
1965	163	23	895
1966	121	15	674
1967	205	30	1,133
1968	118	15	659
1969	205	30	1,134
1970	133	17	735
1971	173	25	955

Year	Mean Estimate	Lower 95% Prediction Limit	Upper 95% Prediction Limit
1972	118	15	659
1973	160	22	882
1974	188	27	1,037
1975	183	27	1,011
1976	70	5	417
1977	61	3	376
1978	191	28	1,057
1979	148	20	817
1980	162	23	893
1981	114	14	636
1982	204	30	1,130
1983	205	30	1,134
1984	148	20	817
1985	94	10	536
1986	164	23	904
1987	100	11	566
1988	74	6	438
1989	142	19	785
1990	72	5	427
1991	102	11	575
1992	101	11	570
1993	197	29	1,088
1994	74	6	440
1995	205	30	1,134
1996	205	30	1,134
1997	135	18	747
1998	205	30	1,134
1999	175	25	963
2000	165	23	908
2001	109	13	612
2002	115	14	642
2003	162	23	891

Table 11F-4. *Eurytemora affinis*–X2 Analysis: Mean and 95% Prediction Limits, Alternative 2

Year	Mean Estimate	Lower 95% Prediction Limit	Upper 95% Prediction Limit
1922	175	25	965
1923	125	16	695
1924	69	5	412
1925	145	20	799
1926	127	16	705
1927	191	28	1,053
1928	159	22	877
1929	75	6	441
1930	114	14	638
1931	64	4	389
1932	99	11	563
1933	79	7	460
1934	82	7	479
1935	162	23	891
1936	158	22	868
1937	170	24	935
1938	205	30	1,134
1939	77	6	452
1940	183	27	1,011
1941	204	30	1,132
1942	189	28	1,041
1943	175	25	966
1944	105	12	589
1945	134	18	739
1946	116	14	646
1947	100	11	566
1948	132	17	732
1949	130	17	721
1950	133	17	734
1951	145	20	801
1952	205	30	1,134
1953	138	18	760
1954	173	25	955
1955	77	6	452

Year	Mean Estimate	Lower 95% Prediction Limit	Upper 95% Prediction Limit
1956	182	26	1,005
1957	149	21	824
1958	205	30	1,133
1959	99	11	562
1960	107	12	601
1961	99	11	562
1962	123	16	685
1963	183	27	1,010
1964	74	6	437
1965	161	23	889
1966	122	15	676
1967	205	30	1,133
1968	118	15	659
1969	205	30	1,134
1970	131	17	724
1971	174	25	957
1972	118	15	659
1973	160	22	882
1974	188	27	1,037
1975	183	27	1,011
1976	70	5	417
1977	61	3	376
1978	191	28	1,056
1979	148	20	817
1980	162	23	893
1981	114	14	635
1982	204	30	1,128
1983	205	30	1,134
1984	147	20	808
1985	94	10	538
1986	164	23	904
1987	100	11	566
1988	74	6	438
1989	142	19	785
1990	72	5	427
1991	102	11	577

Year	Mean Estimate	Lower 95% Prediction Limit	Upper 95% Prediction Limit
1992	101	11	571
1993	197	29	1,087
1994	74	6	440
1995	205	30	1,134
1996	205	30	1,134
1997	136	18	754
1998	205	30	1,134
1999	175	25	963
2000	165	23	908
2001	109	13	612
2002	116	14	645
2003	162	23	891

Table 11F-5. *Eurytemora affinis*–X2 Analysis: Mean and 95% Prediction Limits, Alternative 3

Year	Mean Estimate	Lower 95% Prediction Limit	Upper 95% Prediction Limit
1922	176	25	967
1923	125	16	695
1924	69	5	412
1925	145	20	799
1926	127	16	706
1927	191	28	1,053
1928	161	23	889
1929	75	6	441
1930	114	14	638
1931	64	4	389
1932	99	11	562
1933	78	7	460
1934	83	8	481
1935	162	23	891
1936	158	22	868
1937	170	24	935
1938	205	30	1,134
1939	76	6	448
1940	183	27	1,011

Year	Mean Estimate	Lower 95% Prediction Limit	Upper 95% Prediction Limit
1941	204	30	1,132
1942	189	28	1,041
1943	175	25	966
1944	105	12	589
1945	134	18	739
1946	116	14	646
1947	100	11	566
1948	132	17	729
1949	129	17	716
1950	133	17	735
1951	145	20	798
1952	205	30	1,134
1953	138	18	760
1954	173	25	955
1955	77	6	453
1956	183	27	1,009
1957	148	20	817
1958	205	30	1,133
1959	99	11	562
1960	108	13	608
1961	99	11	562
1962	124	16	686
1963	183	27	1,010
1964	74	6	437
1965	161	23	889
1966	118	14	655
1967	205	30	1,133
1968	118	15	659
1969	205	30	1,134
1970	131	17	724
1971	173	25	955
1972	118	15	659
1973	160	22	882
1974	188	27	1,037
1975	183	27	1,011
1976	70	5	417

Year	Mean Estimate	Lower 95% Prediction Limit	Upper 95% Prediction Limit
1977	61	3	378
1978	189	28	1,044
1979	148	20	817
1980	162	23	893
1981	114	14	638
1982	204	30	1,130
1983	205	30	1,134
1984	148	20	817
1985	94	10	536
1986	164	23	904
1987	100	11	565
1988	74	6	438
1989	143	19	786
1990	72	5	427
1991	102	11	575
1992	101	11	570
1993	197	29	1,089
1994	75	6	441
1995	205	30	1,134
1996	205	30	1,134
1997	135	18	745
1998	205	30	1,134
1999	175	25	963
2000	165	23	908
2001	109	13	612
2002	116	14	646
2003	162	23	891

11F.3 Upstream Sediment Entrainment

Estimates of the percentage of suspended sediment in the Sacramento River that could be entrained by the Project intakes at Red Bluff and Hamilton City were made using previously developed rating curves (Huang and Greimann 2011) and USRDOM daily flow data for upstream and downstream at each intake.

Daily suspended sediment concentration (milligrams per liter) in the Sacramento River immediately upstream of the Red Bluff and Hamilton City intakes was estimated from daily mean river flow (cubic feet per second [cfs]) with the following equations:

- Red Bluff (USRDOM flow output for Sacramento River flow upstream of Tehama-Colusa Canal, 176-ABVRBDIVDA):
    - Flow < 10,000 cfs: Concentration = $0.0000368*\mathrm{Flow}^{1.5}$
    - Flow 10,000–20,000 cfs: Concentration = $2.32\mathrm{E}{-10}*\mathrm{Flow}^{2.8}$
    - Flow > 20,000 cfs: Concentration = $0.34*\mathrm{Flow}^{0.67}$
- Hamilton City (USRDOM flow output for Sacramento River flow upstream of Glenn-Colusa Irrigation District Main Canal, 155-BLW-WOODSO):
    - Flow < 10,000 cfs: Concentration = $8\mathrm{E}{-11}*\mathrm{Flow}^{3}$
    - Flow ≥ 10,000 cfs: Concentration = $0.0002*\mathrm{Flow}^{1.4}$

For all scenarios, suspended sediment concentration at each intake was calculated based on the NAA scenario, to avoid estimating differing suspended sediment concentration because of differences in operations (e.g., reservoir releases, Project diversions). The daily suspended sediment load approaching each intake was calculated as the suspended sediment concentration (from equations above, converted to grams per cubic foot by multiplying by 28.316836) multiplied by the river flow from the USRDOM output locations shown above, multiplied by the number of seconds per day (i.e., 86,400).

The daily amount of suspended sediment load entrained by the intakes was calculated using the above procedure, but instead of river flow being used to estimated suspended sediment load, the diverted water flow was represented as the difference in flow between upstream and downstream of each intake (in this case specific to each scenario, reflecting differences in diversions), where the downstream flow was from the following USRDOM outputs:

- Red Bluff: Sacramento River flow downstream of Tehama-Colusa Canal (175-RDBLFDIVDA)
- Hamilton City: Sacramento River flow downstream of Glenn-Colusa Irrigation District Main Canal (150-GCC-DIV)

The results of the analysis showed the potential for greater sediment entrainment at the Red Bluff and Hamilton City intakes under Alternatives 1, 2, and 3 than the NAA (Tables 11F-6 and 11F-7). Because the greatest suspended sediment load occurs in wetter years, the overall total for the full simulation period (i.e., 1922–2003) was similar to values in wet years. Across all years, at Red Bluff 2.6%–2.7% of suspended sediment was estimated to be entrained under Alternatives 1, 2, and 3 compared to 1.2% under the NAA (Table 11F-6), whereas at Hamilton City 2.1% of suspended sediment was estimated to be entrained under Alternatives 1, 2, and 3 compared to 1.8% under the NAA (Table 11F-7).

Table 11F-6. Mean Percentage of Suspended Sediment Entrained by Water Year Type and Total Percentage Entrained Over Full 82-Year Simulation Period, Red Bluff Intake

Water Year Type	NAA	Alt 1A	Alt 1B	Alt 2	Alt 3
Wet	1.1%	2.2%	2.3%	2.1%	2.4%
Above Normal	1.8%	3.9%	3.7%	3.9%	3.5%
Below Normal	2.8%	5.1%	4.9%	5.1%	4.7%
Dry	2.7%	4.8%	4.5%	4.8%	4.2%
Critically Dry	1.2%	2.0%	2.0%	2.0%	2.0%
Total	1.2%	2.7%	2.6%	2.6%	2.7%

Note: Water year type values are the means of the annual percentage of suspended sediment load diverted. Total is the overall percentage of the sum of suspended sediment load diverted over the 82-year simulation period.

Table 11F-7. Mean Percentage of Suspended Sediment Entrained by Water Year Type and Total Percentage Entrained Over Full 82-Year Simulation Period, Hamilton City Intake

Water Year Type	NAA	Alt 1A	Alt 1B	Alt 2	Alt 3
Wet	1.6%	2.0%	2.0%	1.9%	2.1%
Above Normal	2.8%	3.3%	3.3%	3.3%	3.0%
Below Normal	5.4%	6.0%	6.0%	6.0%	5.4%
Dry	8.5%	8.2%	8.2%	8.3%	7.5%
Critically Dry	12.9%	11.4%	11.2%	11.6%	11.3%
Total	1.8%	2.1%	2.1%	2.1%	2.1%

Note: Water year type values are the means of the annual percentage of suspended sediment load diverted. Total is the overall percentage of the sum of suspended sediment load diverted over the 82-year simulation period.

11F.4 Delta Outflow–Longfin Smelt Abundance Index Analysis

11F.4.1. Development of Statistical Relationship

The potential effect of the Project on longfin smelt was investigated through development of a statistical model relating the longfin smelt fall midwater trawl (FMWT) abundance index to Delta outflow, the FMWT abundance index 2 years earlier (as a representation of parental stock size), and ecological regime (i.e., 1967–1987, pre-*Potamocorbula amurensis* invasion; 1988–2002, post-*P. amurensis* invasion; and 2003–2020, POD; to represent major ecological changepoints in the Delta, e.g., Nobriga and Rosenfield 2016). Total Delta outflow (thousand acre-feet) was summed and examined for March through May and December through May, similar time periods to previous work by Mount et al. (2013:66–69) and Nobriga and Rosenfield (2016).

Twelve log-linear regression models were considered in the analysis. The models were fit using a Bayesian approach implemented in the R statistical computing language (R Core Team 2021) via the *brms* package (Bürkner 2017) with model weights for averaging posterior predictive distributions calculated using the *loo* package (Vehtari et al. 2017): three Markov Chain Monte Carlo chains were run; flat priors were assumed; there was a 2,000-sample warm-up; 10,000 samples were retained from each chain (30,000 samples total from the posterior); and the $\widehat{R}$ <1.01 on estimated parameters indicated sampling converged on the posterior probability distributions for all models.

Preliminary model comparison was performed using leave-one-out cross validation (LOO; Vehtari et al. 2017). Measures of model predictive accuracy using LOO are asymptotically equal to the widely applicable information criteria (WAIC; Watanabe 2010), but in the case of finite data LOO has been shown to be more robust to influential observations like outliers (Vehtari et al. 2017). The preliminary model comparisons indicated there was a relatively high degree of similarity in terms of predictive ability between the top scoring individual models. The extent of model overlap in predictive accuracy was measured by the differences (and the standard errors of the differences) in expected log pointwise predictive densities, i.e., the differences in out-of-sample predictive accuracy between models.

Therefore, rather than selecting a single model for inference, the posterior predictive probability distributions were combined as a weighted average across models. This process involved taking draws from the posterior of each single model in proportion to its model weight. For example, if a single model's weight was 25% of the total model set, then 2,500 draws from its posterior were added to the averaged posterior predictive distribution, which again included 10,000 total draws across all models. The statistical approach used to calculate the model weights for averaging the posterior predictive distributions across models is known as "stacking" (Yao et al. 2018).

Compared to more traditional model averaging approaches, stacking differs in terms of how model weights are assigned. Instead of calculating model weights based on the relative predictive ability for each individual model—where the best model for prediction would be given the highest weight —the model weights estimated through stacking minimize the LOO mean squared error of the resulting averaged posterior predictive distribution across models. In other words, stacking was used to estimate the optimal linear combination of model weights (Yao et al. 2018).

Hence, the model with the largest stacking weight does not necessarily have the highest predictive score compared to other models in the set. For example, the models in this case can be divided into two subsets: one subset includes a covariate for Delta outflow during December–May and the other model subset includes a covariate for March–May Delta outflow (Table 11F-8). Comparing the predictive ability of each individual model using LOO resulted in a model with December–May outflow (the model with the third highest stacking weight in Table 11F-8) having the highest individual predictive accuracy of any single model considered. In contrast, stacking resulted in a model with March–May having the highest single model weight (36% of the total stacking weight). Nevertheless, because stacking optimizes the linear combination of model weights, the next three models (~64% of the stacking weight) all include December–May instead of March–May. Therefore, in this case, even though the model with highest stacking weight included March–May Delta outflow, the averaged posterior predictive distribution was ultimately weighted more heavily with models that include December–May Delta outflow compared to models with March–May Delta outflow. Of the 12 models considered, the top four models by stacking weight accounted for 99.9% of the averaged posterior predictive distribution (Table 11F-8).

Several additional models were also examined, in addition to those in Table 11F-8, but they were ultimately not included in this analysis due to poor model fits and what would have been additional computational cost without an expected difference in results. The additional models included a squared term on Delta outflow and their examination was motivated by the modeling results of Nobriga and Rosenfield (2016). Those authors assessed the relationship between Delta outflow and the ratio of age-0 to age-2 longfin smelt abundance in the two-life-stage versions of the models included in their analyses. They found support for non-linearity in this relationship (i.e., there was a peak in productivity at more intermediate outflow values), which led to the inclusion of a second-order polynomial regression (i.e., a squared term) on Delta outflow (Nobriga and Rosenfield 2016:50). Given the approach taken here, which differs from the Nobriga and Rosenfield analysis in terms of: (1) the survey data used for longfin smelt abundance; (2) how Delta outflow values were included as covariates; and (3) the overall time periods for available data included in the regression models, there was little to no support found for a second-order polynomial regression on Delta outflow. The aforementioned factors that differed between the two analyses are briefly described in the next paragraph for completeness; however, given the poor predictive ability of the second-order polynomial regressions under the current approach, that subset of models was ultimately not included because the preliminary results indicated the stacked model weights would be near zero. Hence the averaged posterior predictive distributions would not be expected to be sensitive to the exclusion of those models in this case, but their inclusion would have increased the computational time necessary to run and perform the averaging over a larger set of models.

As outlined above, there are several differences between these analyses and those of Nobriga and Rosenfield (2016) that might explain the discrepancy in terms of support (or lack thereof) found for dome-shaped longfin smelt productivity as a function of Delta outflow. Firstly, Nobriga and Rosenfield (2016) found support for this relationship fitting models to catch data from the San Francisco Bay Study. In these analyses, on the other hand, the regression models have been fit to the FMWT index of abundance instead. Second, Nobriga and Rosenfield (2016) incorporated covariate values for Delta outflow based on a principal component analysis (the first principal component values) of the z-scored monthly means from December to May. Here, the monthly total outflow (either from December to May, or March to May) were summed, resulting in a total outflow value during each time period each year, and the regression covariate values were calculated as the z-scores of the period-total outflow values taken across years. Third, in addition to examining indices of abundance from different surveys, the annual time periods that have been examined also differ. Nobriga and Rosenfield (2016) examined the relationship between annual indices of longfin smelt abundance-at-age and Delta outflow that were available from the Bay Study during 1980–2013. Whereas in these analyses this relationship was examined over a longer period, during 1967–2020, which includes 20 additional years in the comparison with Delta outflow.

Table 11F-8. The Optimal Linear Combination of Model Weights Based on Stacking, Which Minimizes the Mean Squared Error of the Leave-One-Out Cross Validation for the Resulting Model Averaged Posterior Predictive Distribution across the Twelve Log-Linear Regressions of Longfin Smelt Fall Midwater Trawl Abundance Index. Models are a Function of Delta Outflow (December–May or March–May), Ecological Regime (1967–1987, pre-*Potamocorbula amurensis* invasion; 1988–2002, post-*P. amurensis* invasion; and 2003–2020, Pelagic Organism Decline), and Abundance Index 2 Years Earlier (Log_{10} FMWT(yr – 2))

Log_{10}FMWT Linear Regression Model [1]	Stacking Weight
Mar–May + Regime + Log_{10} FMWT(yr – 2)	0.3583
Dec–May + Regime	0.3154
Dec–May + Regime + Log_{10} FMWT(yr – 2)	0.1995
Dec–May + Log_{10} FMWT(yr – 2)	0.1260
Dec–May + Regime + Dec–May * Regime	0.0006
Dec–May + Regime + Dec–May * Regime + Log_{10} FMWT(yr – 2)	<0.0001
Mar–May + Regime + Mar–May * Regime + Log_{10} FMWT(yr – 2)	<0.0001
Mar–May + Log_{10} FMWT(yr – 2)	<0.0001
Mar–May + Regime	<0.0001
Mar–May + Regime + Mar–May * Regime	<0.0001
Dec–May	<0.0001
Mar–May	<0.0001

[1] An asterisk "*" sign represents an interaction term between regime and Delta outflow.

11F.4.2. Assessment of Project Alternatives

Predictions of the FMWT abundance index under the alternative modeled CALSIM outflow scenarios (1922–2003) were generated using the model stacking approach described above to generate a weighted average Bayesian posterior predictive distribution across the set of models considered. Dropping subscripts denoting individual models for simplicity, the general form of the models can be written as:

$$Log_{10}[FMWT_{yr}] \sim N(\mu_{yr}, \sigma^2) \quad (1)$$

$$\mu_{yr} = \beta_{0,i} + \beta_1 Outflow_{yr,j} + \beta_2 Log_{10}\left[FMWT_{yr-2}\right] + \beta_3 Regime_i * Outflow_{yr,j} \quad (2)$$

Where:

$Log_{10}[FMWT_{yr}]$ is the model predicted Log_{10} value of the FMWT index in water year *yr*;

μ_{yr} is the expected FMWT index in water year *yr* (the stacked posterior predictive distribution for μ_{yr} is shown as the dark gray ribbon in Figure 11F-1);

σ^2 is the residual variance parameter (the stacked posterior predictive distribution including the residual variance is shown as the light gray ribbon in Figure 11F-1);

$\beta_{0,i}$ represents the intercept parameter estimated for each regime: Pre-*Potamocorbula* (i = 1); *Potamocorbula* (i = 2); and POD (i = 3). For models without a regime covariate, a single intercept is estimated across all years instead, i.e., β_0 is substituted for $\beta_{0,i}$;

β_1 represents the slope parameter estimated for the relationship between the FMWT index and Delta outflow;

$Outflow_{yr,j}$ is the normalized[3] outflow level during water year *yr*, and *j* denotes the outflow level during either the December through May, or the March through May period;

β_2 represents the slope parameter estimated for the relationship between the expected FMWT index and the value of that index 2 years prior. For models without the parental stock covariate, $\beta_2 = 0$, and;

β_3 represents the interaction covariate (the difference in slopes) with respect to the estimated effect of outflow on the FMWT index of abundance during different regimes. For models without this interaction term, $\beta_3 = 0$.

[3] Normalized outflow values for each CALSIM scenario were calculated by subtracting the mean and dividing by the standard deviation of observed Delta outflow values (1967–2020).

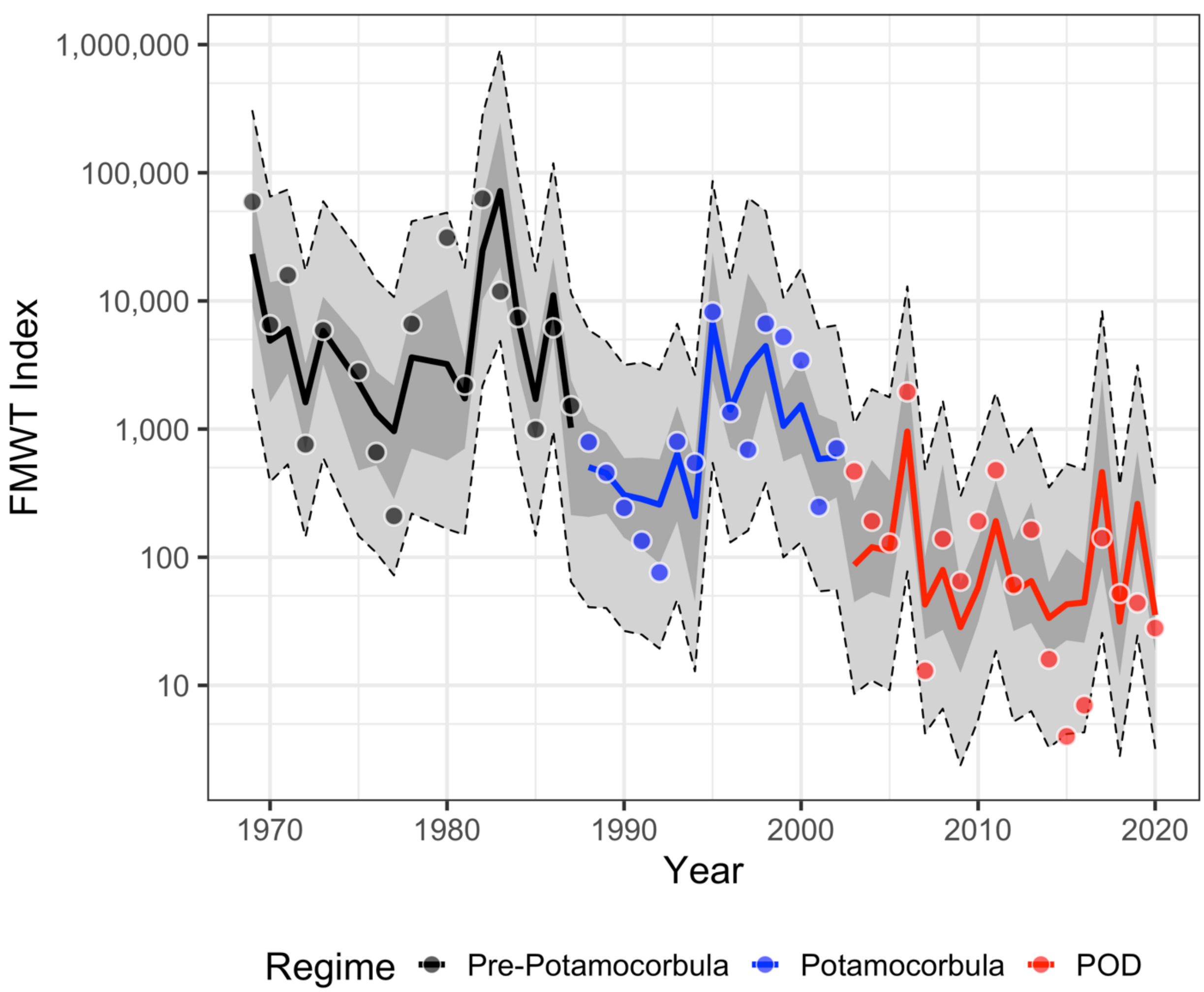

Note: The circles represent the annual historical values of the fall midwater trawl abundance index. The solid lines connect the annual expected values from the stacked Bayesian posterior predictive distribution. Colors correspond to the three modeled regimes. The darker gray ribbon represents the averaged 95% probability interval for draws from the means (in log-space) of the posterior predictive distribution for the fall midwater trawl index value. The lighter gray ribbon with a dashed black outline represents the averaged 95% overall posterior predictive probability interval. The posterior predictive interval for the means has a smaller range than the overall posterior predictive interval because in addition to uncertainty in the estimated mean values, the overall posterior predictive distribution also incorporates uncertainty in the residual error of the model fits (Equations 1 and 2).

Figure 11F-1. Stacked Posterior Predictive Distributions for the Log-Linear Regressions of Longfin Smelt Fall Midwater Trawl Abundance Index as a Function of Delta Outflow (December–May), Ecological Regime (1967–1987, pre-*Potamocorbula amurensis* invasion; 1988–2002, post-*Potamocorbula* invasion [shown as *Potamocorbula*]; and 2003–2020, Pelagic Organism Decline), and Abundance Index 2 Years Earlier [Log10 FMWT(yr – 2)])

For those models that included the Log_{10} FMWT(yr – 2) parental stock size covariate (Table 11F-8), the starting parental stock size in 1922 and 1923 was set at a FMWT index value of 99.4, corresponding to the mean index value from 2011 through 2020. Given the starting values for the FMWT index (in the relevant models), the recursive nature of the regression formula was used to generate the expected FMWT index value in successive years from the posterior predictive distribution 2 years prior. For all models, predictions were conditional on the estimated relationship between the FMWT index and Delta outflow (in December–May, or March–May, depending on the model), and for those models that included a regime covariate, draws from the posterior predictive distributions were conditioned on estimates during the POD regime.

As an example, starting in 1924, draws from the posterior predictive distribution for models including the parental stock size covariate were generated by first substituting the normalized 1924 December through May (or March through May) CALSIM outflow value for each alternative. Draws from the posterior distributions for the regression parameters and the starting value for $Log_{10}[FMWT_{1922}]$ were then used to generate the posterior predictive distribution for the FMWT index in 1924 (μ_{1924}). This value was then substituted into Equation 1, and the posterior distribution for the residual variance parameter was used to generate draws from the pointwise posterior predictive distributions for the FMWT index.[4] This process was iterated over each successive year, substituting the derived μ_{yr-2} values for $Log_{10}[FMWT_{yr-2}]$ to calculate μ_{yr}, and to generate the annual posterior predictive distributions for the FMWT index under each alternative. For models that did not include the parental stock size covariate, the posterior predictive distributions were generated based on the corresponding CALSIM outflow values for the monthly period corresponding to the individual model estimates, and likewise conditioned on covariate estimates during the POD regime for models that included a regime covariate (or the constant intercept parameter β_0, for models without the regime covariate). As noted above in the description of the model stacking approach, draws from the posterior predictive distribution for each model were sampled in proportion to the stacking model weights, to generate a weighted average posterior predictive distribution across the models considered. Summaries were then calculated by grouping the stacked annual posterior predictive distributions by water year type and calculating the means and credible intervals for each aggregated water year type posterior predictive distribution.

11F.5 Delta Outflow–Longfin Smelt Abundance Analysis (Based on Nobriga and Rosenfield 2016)

Nobriga and Rosenfield (2016) examined various formulations of a Ricker (1954) stock-recruitment model to simulate FMWT indices through time. They found that December–May Delta outflow had a positive association with recruits per spawner and that juvenile recruitment from age 0 to age 2 was density dependent (lower survival with greater numbers of juveniles) but

[4] "~*N*" in Eqn. 1 denotes a normal (Gaussian) distribution.

cautioned that the density dependence in the model may be too strong.[5] As described by California Department of Water Resources (2020:4-178), it should also be noted that analyses relying on surveys such as the FMWT index do not fully encompass the range of longfin smelt and do not reflect potential changes in catchability over time because of factors such as increased water clarity and gear avoidance (Latour 2016) that are the subject of ongoing investigations. The model has been retained for this Final EIR/EIS for continuity with the RDEIR/SDEIS, although to address comments on the RDEIR/SDEIS and comments on the analysis based on Nobriga and Rosenfield (2016), the analysis described above in Section 11F.4, *Delta Outflow–Longfin Smelt Abundance Index Analysis* was added and receives greater weight in the consideration of potential impacts.

11F.5.1. Reproduction of Nobriga and Rosenfield (2016) Model

This analysis reproduced the methods described in Nobriga and Rosenfield (2016) for calculation of the two-life-stage model referred to as the “2abc” model, which includes the embedded hypotheses that understanding the trend in age-0 longfin smelt relative abundance requires explicit modeling of spawning and recruit relative abundance, that the production of age-0 fish is density dependent, and that juvenile survival from age 0 to age 2 has changed over time. For purposes of this effects analysis, the “2abc” model was selected because its median predictions visually fit recent years of empirical data better than the other model evaluated.

Model input data used to reproduce the “2abc” model were as provided in Table 2 of Nobriga and Rosenfield (2016). The input data are provided in Appendix A of Greenwood and Phillis (2018). The analyses were run in R software (R Core Team 2021).

Graphical comparison of the reproduction of the “2abc” model to the original Nobriga and Rosenfield (2016) “2abc” model (Figure 11F-2 and Figure 11F-3) suggests that the reproduced model was a reasonable approximation of the original model (i.e., the reproduction of the method was reasonably successful). It should be noted that the original “2abc” model 95% confidence intervals are wider than the reproduction utilized in this analysis. However, the model coefficients and standard errors are identical between the original and reproduced models. Therefore, the reproduced “2abc” model utilized in this analysis is considered appropriate, and the differences in 95% confidence intervals among the original and reproduced models do not affect the comparison of the scenarios discussed below.

[5] Comments on the draft Environmental Impact Report for Long-Term Operation of the California State Water Project suggested that a form of stock-recruitment function other than the Ricker method used by Nobriga and Rosenfield (2016) would be appropriate for exploration, such as the Beverton-Holt method (California Department of Water Resources 2020:4-178). The Beverton-Holt method was explored for the Final EIR but was found to be a poorer fit to the empirical data than the Ricker method, so the Ricker method consistent with Nobriga and Rosenfield (2016) was retained (California Department of Water Resources 2020:4-178). For the present impact analysis of Alternatives 1, 2, and 3 compared to the NAA, the Ricker method was also retained, consistent with California Department of Water Resources (2020) and Nobriga and Rosenfield (2016).

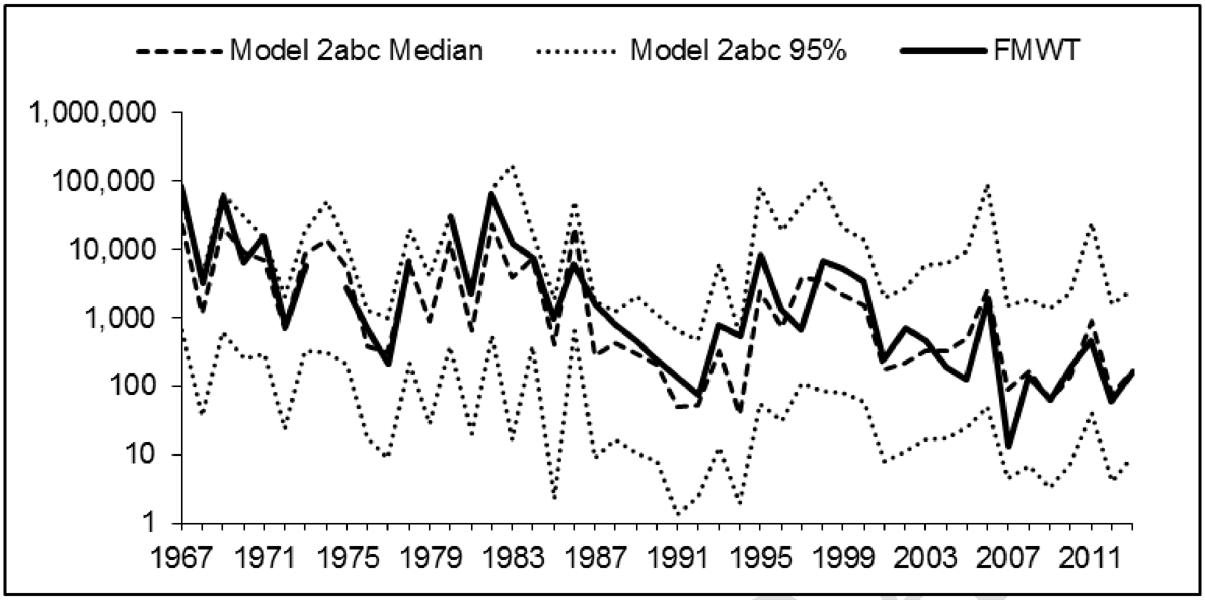

Source: California Department of Water Resources 2020:E-86.
FMWT = fall midwater trawl.

Figure 11F-2. Reproduction of Nobriga and Rosenfield (2016) 2abc Model Predictions Compared to Historical Fall Midwater Trawl Survey Longfin Smelt Abundance Index.

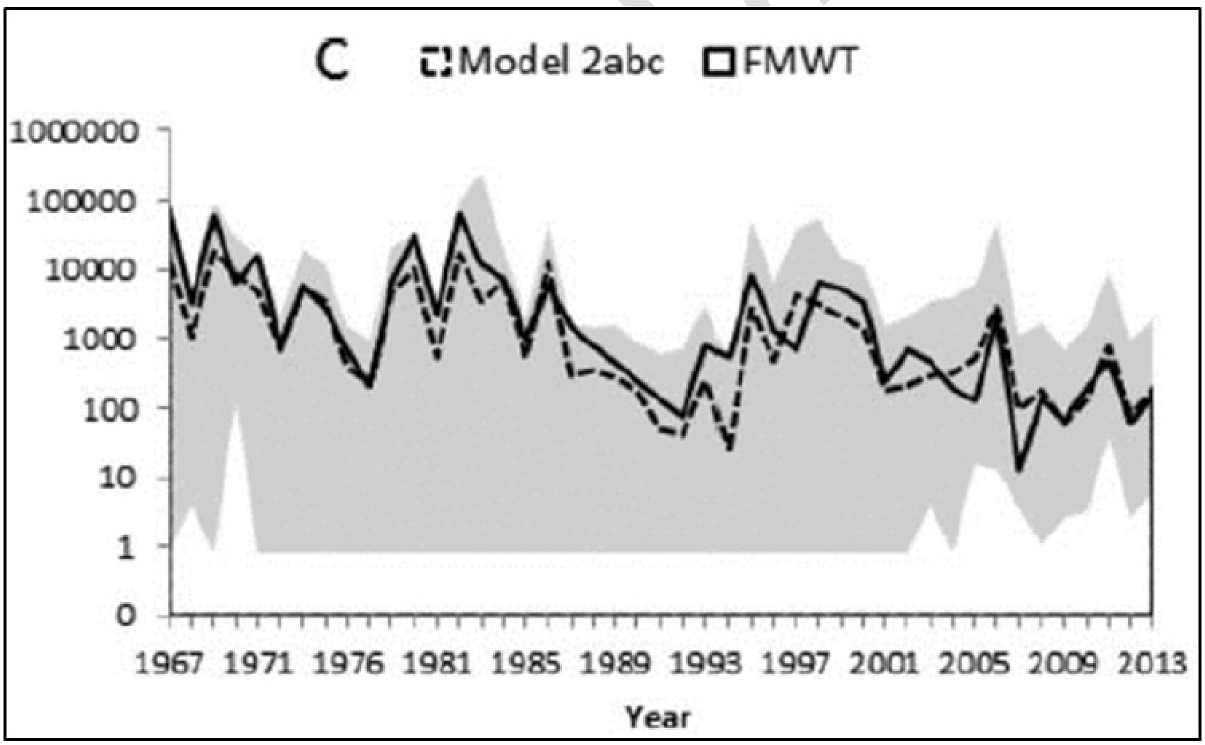

Source: California Department of Water Resources 2020:E-86.
Gray shading indicates 95% interval.
FMWT = fall midwater trawl.

Figure 11F-3. Original (Figure 6c of Nobriga and Rosenfield 2016) 2abc Model Predictions Compared to Historical Fall Midwater Trawl Survey Longfin Smelt Abundance Index.

11F.5.2. Calculation of Delta Outflow Model Inputs for Scenario Comparison

To obtain the required first principal component (PC1) model inputs for comparison of the NAA and Alternative 1–3 scenarios, it was first necessary to reproduce the principal components analysis (PCA). Following Nobriga and Rosenfield (2016), historical daily Delta outflow data were acquired from the DAYFLOW database.[6] Flow data were averaged for December to May by month and year and the principal component analysis was conducted using the 'PCA' function in the R package FactoMineR (Le et al. 2008) on water years 1956–2013. The resulting PC1 outputs were very similar to the original values computed by Nobriga and Rosenfield (2016), suggesting that the reported method had been successfully reproduced.[7] The 'predict PCA' function was then used to predict PC1 values for the NAA and Alternative 1–3 scenarios for water years 1922–2003 based on the CALSIM modeling of the scenarios, on the same projection as the PCA. The resulting PC1 values were used as the input for the model simulation of the flow scenarios described in the next section.

11F.5.3. Model Simulation to Compare Scenarios

Model simulation to compare the NAA and Alternative 1–3 scenarios used the PC1 flow inputs. To produce a simulation for the 1922–2003 time series, and consistent with Nobriga and Rosenfield (2016), the model was initiated with 2 years (i.e., years 1922 and 1923) of FMWT indices equal to 798, which represents the median observed FMWT index from 1967 to 2013. The simulation was conducted for two juvenile survival functions:

- 'good,' which used the pre-1991 relatively high survival for simulation over the full 1922–2003 time series;
- 'poor,' which used the post-1991 relatively low survival for simulation over the full 1922–2003 simulation time series.

Following Nobriga and Rosenfield (2016), 1,000 stochastic simulations were conducted in which random draws were made based on the mean and standard error of the model parameters. Consistent with Nobriga and Rosenfield (2016), the variability among the estimates was examined using the 95% intervals. Results of the analysis are summarized in the main body of Chapter 11, *Aquatic Biological Resources*.

11F.6 X2–Longfin Smelt Abundance Index Analysis

The method is the same as that used recently by California Department of Water Resources (2020). The methods described herein are the same as those used in that application; the methods description below was adapted from California Department of Water Resources (2020:E2-1).

---

[6] https://www.water.ca.gov/Programs/Environmental-Services/Compliance-Monitoring-And-Assessment/Dayflow-Data

[7] The small differences may have arisen because of varying PCA algorithms in different statistical software packages, for example.

The analysis essentially updated previously described X2-abundance index regressions (Kimmerer et al. 2009, Mount et al. 2013) by adding additional years of data. Updating the analysis allowed full accounting of sources of error in the predictions, allowing calculation of prediction intervals from estimates of X2, as recommended by Simenstad et al. (2016), for the NAA and Alternative 1–3 scenarios.

Longfin smelt FMWT index data were obtained (http://www.dfg.ca.gov/delta/data/fmwt/indices.asp?view=single), including indices for 1967–2014 (excluding 1974 and 1979, when there was no sampling). For each index year, mean X2 during January–June was calculated based on X2 from the DAYFLOW database (https://data.cnra.ca.gov/dataset/dayflow), in addition to calculated X2 for earlier years.[8]

Similar to Mount et al. (2013), GLMs were run, predicting longfin smelt FMWT relative abundance index as a function of X2 and step changes in 1987/1988 and 2002/2003:

$$\mathrm{Log}_{10}(\mathrm{FMWT\ index}_{y}) = a + b\cdot(\mathrm{mean\ X2}_{y}) + c\cdot\mathrm{period}_{y}$$

Where y indicates year, a is the intercept, b is the coefficient applied to the mean Delta outflow, and c takes one of three values for period: 0 for the pre-*Potamocorbula* period (1967–1987), and values to be estimated for post-*Potamocorbula* (1988–2002) and POD (2003–2014) periods.

Regarding the months used for mean X2, Mount et al. (2013:67) noted the following:

> The months selected in the original analysis [by Jassby et al. 1995] were based on the assumption that the (unknown) X2 mechanism operated during early life history of Longfin Smelt, which smelt experts linked to this period. Autocorrelation in the X2 values through months means that statistical analysis provides little guidance for improving the selection of months. A better understanding of the mechanism(s) underlying the relationship would probably allow this period to be narrowed and focused, but for now there is little basis for selecting a narrower period for averaging X2.

Mount et al. (2013) compared the fit of X2 averaging periods for January–June (i.e., the original period used by Jassby et al. 1995, also used by Kimmerer et al. 2009) and March–May; they selected the former because the fit to the empirical data was slightly superior. In the present analysis, both the January–June and March–May averaging periods were compared for their adequacy of fit, using standard criteria (Akaike's Information Criterion adjusted for small sample sizes, AIC_c; and variation explained, r^2). This showed that the January–June X2 averaging period was better supported in terms of explaining variability in the FWMT index (Table 11F-9; Figure 11F-4), so this averaging period was used in the subsequent comparison of the NAA and Alternative 1–3 scenarios based on DSM2 outputs of X2.

[8] DAYFLOW provides X2 estimates from water year 1997 onwards, so the DAYFLOW equation (X2(t) = 10.16 + 0.945*X2(t-1) – 1.487log(QOUT(t))) was used to provide X2 for earlier years, based on a starting unpublished estimate of X2 (Mueller-Solger 2012 as cited by Greenwood [2018: 3]).

Table 11F-9. Parameter Coefficients for General Linear Models Explaining Longfin Smelt Fall Midwater Trawl Index as a Function of Mean January–June and March–May X2 and Step Changes in 1987/1988 (*Potamocorbula* Invasion) and 2002/2003 (Pelagic Organism Decline).

Parameter	January–June Estimate	January–June Standard Error	January–June *P*	March–May Estimate	March–May Standard Error	March–May *P*
a (Intercept)	7.3059	0.3299	< 0.0001	6.8100	0.3224	< 0.0001
b (X2)	-0.0542	0.0049	< 0.0001	-0.0475	0.0047	< 0.0001
c (Period: Post-*Potamocorbula*)	-0.5704	0.1174	< 0.0001	-0.6368	0.1271	< 0.0001
c (Period: POD)	-1.4067	0.1244	< 0.0001	-1.4581	0.1351	< 0.0001
Fit	-	-	-	-	-	-
AIC$_c$[1]	-47.4904	-47.4904	-47.4904	-39.5492	-39.5492	-39.5492
r^2	0.8666	0.8666	0.8666	0.8414	0.8414	0.8414

Note:

[1] The difference of ~8 AIC$_c$ units between the two GLMs indicates that the January–June mean X2 GLM is better supported in terms of explaining the patterns in the data (Burnham et al. 2011).

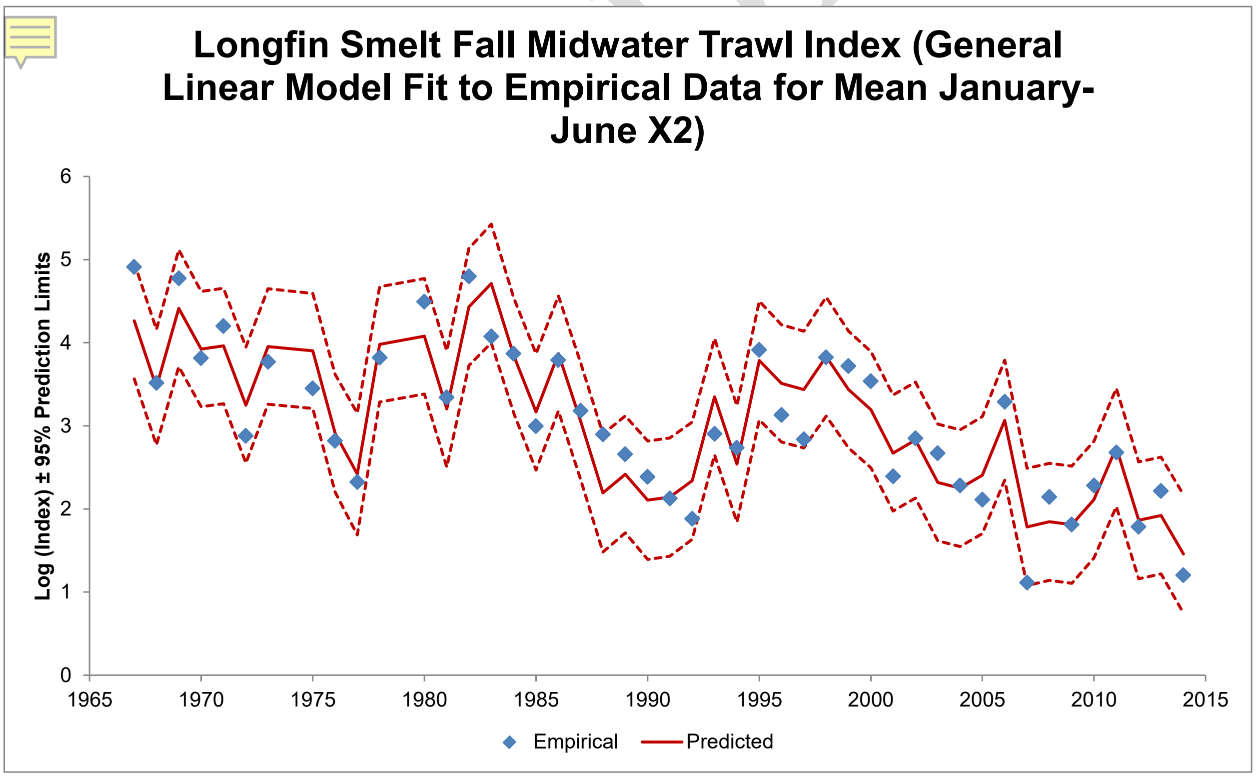

Source: California Department of Water Resources 2020:E2-3.

Figure 11F-4. Fit to Empirical Data of General Linear Model Predicting Longfin Smelt Fall Midwater Trawl Relative Abundance Index as a Function of Mean January–June X2 and Step Changes for *Potamocorbula* and Pelagic Organism Decline.

For the comparison of the NAA and Alternative 1–3 scenarios, mean January–June X2 was calculated for each year of the 1922–2003 simulation based on DSM2 X2 outputs. The X2-abundance index GLM calculated as above was used to estimate abundance index for the scenarios, based on the POD period coefficient in addition to the intercept and X2 slope terms. The basic equation used was (see also Table 11F-9):

$$\log_{10}(\text{Longfin Smelt FMWT index}) = 7.3059 - 0.0542*(\text{January–June X2}) - 1.4067$$

The log-transformed abundance indices were back-transformed to a linear scale for comparison of scenarios. In order to illustrate the variability in predictions from the X2-abundance index GLM, annual estimates were made for the mean and upper and lower 95% prediction limits of the abundance indices, as recommended by Simenstad et al. (2016). Statistical analyses were conducted with PROC GLM and PROC PLM in SAS/STAT software, Version 9.4 of the SAS System for Windows.[9]

Results of the analysis are summarized in the main body of Chapter 11, *Aquatic Biological Resources*. Tables 11F-10 through 11F-14 provide supplemental information also discussed in the main body of Chapter 11.

Table 11F-10. X2–Longfin Smelt Abundance Index Analysis: Mean and 95% Prediction Limits, NAA

Year	Mean Estimate	Lower 95% Prediction Limit	Upper 95% Prediction Limit
1922	351	61	1,824
1923	168	25	886
1924	12	-6	102
1925	147	21	783
1926	110	14	593
1927	523	94	2,727
1928	188	29	991
1929	21	-4	150
1930	92	10	504
1931	9	-6	88
1932	84	9	466
1933	24	-3	164
1934	42	0	254
1935	218	35	1,140
1936	306	52	1,596

[9] Copyright 2002–2012, SAS Institute Inc. SAS and all other SAS Institute Inc. product or service names are registered trademarks or trademarks of SAS Institute Inc., Cary, NC, USA

Year	Mean Estimate	Lower 95% Prediction Limit	Upper 95% Prediction Limit
1937	217	35	1,136
1938	798	145	4,190
1939	18	-5	136
1940	365	64	1,898
1941	733	133	3,844
1942	690	125	3,615
1943	439	78	2,282
1944	60	4	342
1945	132	18	707
1946	170	26	899
1947	45	1	269
1948	107	13	580
1949	66	5	374
1950	153	22	810
1951	311	53	1,619
1952	891	162	4,693
1953	323	56	1,682
1954	278	47	1,450
1955	37	-1	229
1956	635	115	3,322
1957	116	15	626
1958	744	135	3,902
1959	96	11	526
1960	58	3	333
1961	58	3	334
1962	102	12	555
1963	368	64	1,915
1964	35	-1	220
1965	397	70	2,064
1966	138	19	733
1967	894	163	4,710
1968	128	17	686
1969	868	158	4,572
1970	251	42	1,310
1971	455	81	2,371
1972	77	7	428

Year	Mean Estimate	Lower 95% Prediction Limit	Upper 95% Prediction Limit
1973	402	71	2,090
1974	591	107	3,086
1975	313	54	1,632
1976	10	-6	96
1977	6	-7	72
1978	551	99	2,872
1979	207	33	1,085
1980	417	74	2,172
1981	92	10	502
1982	765	139	4,017
1983	927	169	4,890
1984	300	51	1,561
1985	48	1	285
1986	283	48	1,474
1987	46	1	272
1988	39	0	241
1989	69	6	390
1990	20	-4	144
1991	26	-3	174
1992	48	1	284
1993	698	127	3,657
1994	22	-4	156
1995	879	160	4,632
1996	670	121	3,504
1997	281	47	1,465
1998	863	157	4,543
1999	447	79	2,326
2000	267	45	1,395
2001	68	5	384
2002	155	23	821
2003	385	68	2,003

Table 11F-11. X2–Longfin Smelt Abundance Index Analysis: Mean and 95% Prediction Limits, Alternative 1A

Year	Mean Estimate	Lower 95% Prediction Limit	Upper 95% Prediction Limit
1922	343	59	1,785
1923	168	25	885
1924	12	-6	104
1925	148	21	788
1926	108	13	584
1927	496	89	2,586
1928	183	28	965
1929	21	-4	150
1930	90	10	495
1931	9	-6	88
1932	82	8	452
1933	24	-3	164
1934	43	0	260
1935	209	33	1,097
1936	304	52	1,584
1937	214	34	1,120
1938	794	145	4,173
1939	18	-5	135
1940	359	63	1,867
1941	733	133	3,841
1942	690	125	3,615
1943	438	78	2,279
1944	59	4	341
1945	143	20	760
1946	168	25	889
1947	45	1	270
1948	108	13	585
1949	63	5	361
1950	152	22	807
1951	311	53	1,617
1952	891	163	4,694
1953	323	56	1,681
1954	265	44	1,382
1955	37	-1	230

Year	Mean Estimate	Lower 95% Prediction Limit	Upper 95% Prediction Limit
1956	629	114	3,287
1957	112	14	606
1958	732	133	3,839
1959	93	10	509
1960	56	3	324
1961	55	3	320
1962	100	12	545
1963	362	63	1,881
1964	35	-1	219
1965	392	69	2,042
1966	135	19	720
1967	890	162	4,690
1968	127	17	681
1969	867	158	4,567
1970	248	41	1,294
1971	455	81	2,370
1972	74	7	414
1973	401	71	2,084
1974	591	107	3,087
1975	312	53	1,623
1976	10	-6	96
1977	5	-7	70
1978	568	102	2,963
1979	203	32	1,065
1980	415	73	2,160
1981	87	9	479
1982	765	139	4,017
1983	927	169	4,890
1984	300	51	1,562
1985	48	1	284
1986	283	48	1,474
1987	44	1	263
1988	37	-1	228
1989	67	5	381
1990	20	-4	145
1991	25	-3	169

Year	Mean Estimate	Lower 95% Prediction Limit	Upper 95% Prediction Limit
1992	47	1	279
1993	688	125	3,602
1994	22	-4	152
1995	870	159	4,583
1996	661	120	3,459
1997	281	47	1,465
1998	856	156	4,504
1999	446	79	2,324
2000	263	44	1,373
2001	65	5	372
2002	151	22	804
2003	379	66	1,972

Table 11F-12. X2–Longfin Smelt Abundance Index Analysis: Mean and 95% Prediction Limits, Alternative 1B

Year	Mean Estimate	Lower 95% Prediction Limit	Upper 95% Prediction Limit
1922	343	59	1,785
1923	168	25	888
1924	12	-6	104
1925	147	21	780
1926	108	13	584
1927	497	89	2,588
1928	183	28	964
1929	21	-4	150
1930	90	10	495
1931	9	-6	88
1932	82	8	452
1933	24	-3	164
1934	43	0	260
1935	209	33	1,097
1936	304	52	1,584
1937	213	34	1,118
1938	794	145	4,173
1939	17	-5	130
1940	359	62	1,867

Year	Mean Estimate	Lower 95% Prediction Limit	Upper 95% Prediction Limit
1941	733	133	3,842
1942	690	125	3,615
1943	438	78	2,279
1944	59	4	341
1945	132	18	705
1946	168	25	889
1947	45	1	271
1948	108	13	585
1949	63	5	361
1950	152	22	806
1951	310	53	1,616
1952	891	163	4,694
1953	323	56	1,681
1954	265	44	1,381
1955	37	-1	231
1956	630	114	3,291
1957	113	14	608
1958	717	130	3,759
1959	93	10	509
1960	57	3	329
1961	60	4	345
1962	100	12	545
1963	362	63	1,882
1964	35	-1	218
1965	401	71	2,084
1966	127	17	681
1967	889	162	4,686
1968	127	17	681
1969	868	158	4,570
1970	257	43	1,342
1971	457	81	2,379
1972	74	7	413
1973	400	70	2,079
1974	591	107	3,087
1975	312	53	1,623
1976	10	-6	95

Year	Mean Estimate	Lower 95% Prediction Limit	Upper 95% Prediction Limit
1977	5	-7	70
1978	568	102	2,964
1979	203	32	1,065
1980	415	73	2,161
1981	87	9	479
1982	765	139	4,017
1983	927	169	4,890
1984	311	53	1,619
1985	47	1	281
1986	283	48	1,477
1987	44	1	263
1988	37	-1	227
1989	67	5	377
1990	20	-4	145
1991	25	-3	168
1992	47	1	277
1993	689	125	3,607
1994	22	-4	152
1995	871	159	4,585
1996	661	120	3,459
1997	276	47	1,440
1998	857	156	4,512
1999	446	79	2,324
2000	263	44	1,373
2001	66	5	372
2002	152	22	806
2003	379	66	1,972

Table 11F-13. X2–Longfin Smelt Abundance Index Analysis: Mean and 95% Prediction Limits, Alternative 2

Year	Mean Estimate	Lower 95% Prediction Limit	Upper 95% Prediction Limit
1922	343	59	1,785
1923	168	25	885
1924	12	-6	104
1925	148	21	788

Year	Mean Estimate	Lower 95% Prediction Limit	Upper 95% Prediction Limit
1926	108	13	584
1927	496	89	2,586
1928	183	28	965
1929	21	-4	150
1930	90	10	496
1931	9	-6	88
1932	81	8	452
1933	24	-3	164
1934	43	0	259
1935	209	33	1,097
1936	305	52	1,590
1937	214	34	1,119
1938	794	145	4,173
1939	18	-5	135
1940	359	63	1,867
1941	733	133	3,842
1942	690	125	3,615
1943	438	78	2,279
1944	59	4	341
1945	143	20	760
1946	168	25	889
1947	45	1	270
1948	108	13	585
1949	63	5	361
1950	152	22	805
1951	311	53	1,617
1952	891	163	4,694
1953	323	56	1,681
1954	265	44	1,383
1955	37	-1	230
1956	629	114	3,287
1957	112	14	607
1958	732	133	3,839
1959	93	10	509
1960	56	3	324
1961	55	3	320

Year	Mean Estimate	Lower 95% Prediction Limit	Upper 95% Prediction Limit
1962	100	12	545
1963	362	63	1,881
1964	35	-1	219
1965	392	69	2,041
1966	134	18	713
1967	890	162	4,690
1968	127	17	681
1969	867	158	4,567
1970	248	41	1,294
1971	455	81	2,370
1972	74	7	414
1973	401	71	2,084
1974	591	107	3,087
1975	312	53	1,623
1976	10	-6	96
1977	5	-7	70
1978	567	102	2,961
1979	203	32	1,065
1980	415	73	2,160
1981	87	9	479
1982	765	139	4,017
1983	927	169	4,890
1984	300	51	1,562
1985	48	1	284
1986	283	48	1,474
1987	44	1	263
1988	37	-1	228
1989	69	6	388
1990	20	-4	145
1991	25	-3	170
1992	47	1	278
1993	688	125	3,604
1994	22	-4	152
1995	870	159	4,583
1996	661	120	3,459
1997	281	47	1,465

Year	Mean Estimate	Lower 95% Prediction Limit	Upper 95% Prediction Limit
1998	856	156	4,504
1999	446	79	2,324
2000	263	44	1,374
2001	65	5	372
2002	151	22	804
2003	379	66	1,971

Table 11F-14. X2–Longfin Smelt Abundance Index Analysis: Mean and 95% Prediction Limits, Alternative 3

Year	Mean Estimate	Lower 95% Prediction Limit	Upper 95% Prediction Limit
1922	343	59	1,783
1923	167	25	882
1924	12	-6	104
1925	148	21	785
1926	108	13	585
1927	498	89	2,594
1928	190	30	999
1929	21	-4	148
1930	90	10	494
1931	9	-6	89
1932	81	8	449
1933	24	-3	164
1934	43	0	260
1935	209	33	1,097
1936	306	52	1,591
1937	213	34	1,116
1938	794	145	4,173
1939	17	-5	131
1940	358	62	1,861
1941	733	133	3,842
1942	690	125	3,615
1943	438	78	2,279
1944	59	4	341
1945	145	21	771
1946	168	25	890

Year	Mean Estimate	Lower 95% Prediction Limit	Upper 95% Prediction Limit
1947	44	1	263
1948	104	13	565
1949	61	4	351
1950	151	22	802
1951	309	53	1,607
1952	891	163	4,695
1953	323	56	1,681
1954	265	44	1,381
1955	40	0	243
1956	633	115	3,310
1957	109	14	591
1958	713	130	3,737
1959	93	10	508
1960	58	3	333
1961	56	3	323
1962	100	12	547
1963	362	63	1,881
1964	35	-1	218
1965	393	69	2,042
1966	121	16	648
1967	885	161	4,660
1968	127	17	680
1969	870	159	4,580
1970	250	41	1,306
1971	457	81	2,380
1972	74	7	413
1973	400	70	2,079
1974	591	107	3,083
1975	312	53	1,624
1976	10	-6	95
1977	6	-7	73
1978	551	99	2,875
1979	202	32	1,061
1980	416	73	2,162
1981	88	9	482
1982	765	139	4,017

Year	Mean Estimate	Lower 95% Prediction Limit	Upper 95% Prediction Limit
1983	927	169	4,890
1984	311	53	1,619
1985	47	1	281
1986	299	51	1,559
1987	44	1	262
1988	37	-1	227
1989	69	6	390
1990	20	-4	144
1991	25	-3	168
1992	46	1	276
1993	690	125	3,615
1994	22	-4	153
1995	871	159	4,584
1996	661	120	3,460
1997	275	46	1,434
1998	858	156	4,515
1999	446	79	2,324
2000	263	44	1,372
2001	65	5	372
2002	153	22	811
2003	380	67	1,976

11F.7 Tidal Habitat Restoration Mitigation Calculations for Longfin Smelt

Tidal habitat restoration mitigation for longfin smelt was calculated based on the same method recently applied by California Department of Water Resources (2019:5-5). The method applied is that of Kratville (2010), who combined statistical relationships between export:inflow (E:I) ratio and proportion of particles entrained from various particle injection locations included in DSM2-PTM runs by Kimmerer and Nobriga (2008) with areas of habitat represented by groups of particle injection locations. The logistic equations for these particle injection locations that were applied in the analysis to mean CALSIM-modeled E:I during February–June were as follows (Nobriga pers. comm.; see Kratville 2010 for further explanation of station codes):

- Antioch: Proportional entrainment = $1-(1/(1+0.00271028300855596*e^{6.84578776491213*E:I}))$
- Bacon Island: Proportional entrainment = $1-(1/(1+0.00360067831643248*e^{48.0279532945984*E:I}))$

- Collinsville: Proportional entrainment = $1-(1/(1+0.00122681735447479*e^{7.34600447344753*E:I}))$
- Franks Tract East: Proportional entrainment = $1-(1/(1+0.0882721350895259*e^{6.51283857598075*E:I}))$
- Franks West: Proportional entrainment = $1-(1/(1+0.0321221161869743*e^{5.5544157874989*E:I}))$
- Georgiana Slough: Proportional entrainment = $1-(1/(1+0.0556193254426028*e^{7.53188118299606*E:I}))$
- Hood: Proportional entrainment = $1-(1/(1+0.0370940945312037*e^{6.00721899458561*E:I}))$
- Medford Island: Proportional entrainment = $1-(1/(1+0.00592509281258315*e^{34.8002358833536*E:I}))$
- Mossdale: Proportional entrainment = $1-(1/(1+0.111111111111111*e^{26.6493233888825*E:I}))$
- North Fork Mokelumne: Proportional entrainment = $1-(1/(1+0.0610234435346189*e^{7.28620279196804*E:I}))$
- Potato Slough: Proportional entrainment = $1-(1/(1+0.0163841512024925*e^{23.708308398635*E:I}))$
- Rio Vista: Proportional entrainment = $1-(1/(1+0.0076755045686138*e^{6.69498358561645*E:I}))$
- Ryde: Proportional entrainment = $1-(1/(1+0.0117017438595754*e^{6.7207341005591*E:I}))$
- South Fork Mokelumne: Proportional entrainment = $1-(1/(1+0.0389615268878375*e^{14.4737516748024*E:I}))$
- Stockton: Proportional entrainment = $1-(1/(1+0.00840706847099802*e^{32.6988703978096*E:I}))$
- Three Mile Slough: Proportional entrainment = $1-(1/(1+0.0157935505682666*e^{6.10724605041376*E:I}))$
- Twitchell Island: Proportional entrainment = $1-(1/(1+0.0342441647821108*e^{6.37831755748149*E:I}))$
- Vernalis: Proportional entrainment = $1-(1/(1+0.111111111111111*e^{27.3073879175582*E:I}))$
- Victoria Canal: Proportional entrainment = $1-(1/(1+0.0000001283874368*e^{219.722457733622*E:I}))$

The mean estimate of particle proportional entrainment from application of these equations was calculated for four geographic zones, with this mean estimate of particle entrainment then being multiplied by the area of each zone:

- Lower Sacramento (Antioch, Collinsville, Rio Vista, Ryde, Three Mile Slough): 19,140.69 acres
- Hood and West Dela San Joaquin (Hood, Twitchell Island): 6,080.929 acres
- Georgiana Slough/North Fork Mokelumne (Georgiana Slough, North Fork Mokelumne): 2,704.28 acres

- San Joaquin (Bacon Island, Franks Tract East, Franks Tract West, Medford Island, Mossdale, Potato Slough, South Fork Mokelumne, Stockton, Vernalis, Victoria Canal): 21,124.31 acres

The overall area of effect for each scenario was calculated as 10% of the area of the above calculations, consistent with calculations for the mitigation requirements used by California Department of Fish and Game (2009) and California Department of Water Resources (2019). Results of the mitigation calculations for the number of acres that Alternatives 1–3 were in excess of NAA are provided in the main body of Chapter 11, *Aquatic Biological Resources*.

11F.8 References Cited

11F.8.1. Printed References

Bürkner, P.-C. 2017. *brms*: An R Package for Bayesian Multilevel Models Using Stan. *Journal of Statistical Software* 80(1):1–28.

Burnham, K. P., D. R. Anderson, and K. P. Huyvaert. 2011. AIC Model Selection and Multimodel Inference in Behavioral Ecology: Some Background, Observations, and Comparisons. *Behavioral Ecology and Sociobiology* 65(1):23–35.

California Department of Fish and Game. 2009. *California Endangered Species Act Incidental Take Permit No. 2081-2009-001-03. Department of Water Resources California State Water Project Delta Facilities and Operations*. Yountville, CA: California Department of Fish and Game, Bay Delta Region.

California Department of Fish and Wildlife. 2018. *Zooplankton Study Clarke-Bumpus Net Data, 1972-2017* (file <1972-2017CBMatrix.xlsx>). Available: ftp://ftp.dfg.ca.gov/IEP_Zooplankton/. Accessed: June 4, 2018.

California Department of Water Resources. 2019. *Incidental Take Permit Application for Long-Term Operation of the California State Water Project*. December 13. Available: https://water.ca.gov/-/media/DWR-Website/Web-Pages/Programs/State-Water-Project/Files/1_DWR_LTO_ITP_Application_2019-12-13_a_y19.pdf. Accessed: February 24, 2020.

California Department of Water Resources. 2020. *Final Environmental Impact Report for Long-term Operation of the California State Water Project*. State Clearinghouse No. 2019049121. March.

Greenwood, M. 2018. *Potential Effects on Zooplankton from California WaterFix Operations*. Technical Memorandum to California Department of Water Resources. July 2. Available: https://www.waterboards.ca.gov/waterrights/water_issues/programs/bay_delta/california_waterfix/exhibits/docs/petitioners_exhibit/dwr/part2_rebuttal/dwr_1349.pdf. Accessed: November 30, 2018.

Greenwood, M., and C. Phillis. 2018. *Comparison of Predicted Longfin Smelt Fall Midwater Trawl Index for Existing Conditions, No Action Alternative, and California WaterFix CWF H3+ Operational Scenarios Using the Nobriga and Rosenfield (2016) Population Dynamics Model*. Technical Memorandum to California Department of Water Resources. Sacramento, CA: ICF. Available: https://www.waterboards.ca.gov/waterrights/water_issues/programs/bay_delta/california_waterfix/exhibits/docs/petitioners_exhibit/dwr/part2_rebuttal/dwr_1352.pdf. Accessed: September 24, 2019.

Huang, J. V., and B. Greimann. 2011. *Sediment Loads at Tehama-Colusa, Glen-Colusa, and Delevan Diversions*. Technical Report No. SRH-2011-22. Mid Pacific Region NODOS Investigation Report. June. Denver, CO: U.S. Bureau of Reclamation, Technical Service Center, Sedimentation and River Hydraulics Group.

Jassby, A. D., W. J. Kimmerer, S. G. Monismith, C. Armor, J. E. Cloern, T. M. Powell, J. R. Schubel, and T. J. Vendlinski. 1995. Isohaline Position as a Habitat Indicator for Estuarine Populations. *Ecological Applications* 5(1):272–289.

Kimmerer, W. J. 2002. Effects of Freshwater Flow on Abundance of Estuarine Organisms: Physical Effects or Trophic Linkages? *Marine Ecology Progress Series* 243:39–55.

Kimmerer, W. J., E. S. Gross, and M. L. MacWilliams. 2009. Is the Response of Estuarine Nekton to Freshwater Flow in the San Francisco Estuary Explained by Variation in Habitat Volume? *Estuaries and Coasts* 32(2):375–389.

Kimmerer, W. J., and M. L. Nobriga. 2008. Investigating Particle Transport and Fate in the Sacramento–San Joaquin Delta Using a Particle Tracking Model. *San Francisco Estuary and Watershed Science* 6(1).

Kratville, D. 2010. *California Department of Fish and Game Rationale for Effects of Exports*. California Department of Fish and Game, Sacramento, CA.

Latour, R. J. 2016. Explaining Patterns of Pelagic Fish Abundance in the Sacramento–San Joaquin Delta. *Estuaries and Coasts* 39(1):233–247.

Le, S., J. Josse, and F. Husson. 2008. FactoMineR: An R Package for Multivariate Analysis. *Journal of Statistical Software* 25(1):1–18.

Mount, J., W. Fleenor, B. Gray, B. Herbold, and W. Kimmerer. 2013. *Panel Review of the Draft Bay-Delta Conservation Plan*. Prepared for the Nature Conservancy and American Rivers. September. Saracino & Mount, LLC, Sacramento, CA.

Nobriga, M. L., and J. A. Rosenfield. 2016. Population Dynamics of an Estuarine Forage Fish: Disaggregating Forces Driving Long-Term Decline of Longfin Smelt in California's San Francisco Estuary. *Transactions of the American Fisheries Society* 145(1):44–58.

R Core Team. 2021. *R: A Language and Environment for Statistical Computing*. R Foundation for Statistical Computing, Vienna, Austria. Available: https://www.Rproject.org/.

Ricker, W. E. 1954. Stock and Recruitment. *Journal of the Fisheries Research Board of Canada* 11(5):559–623.

Schemel, L. E. 2001. Simplified Conversions between Specific Conductance and Salinity Units for Use with Data from Monitoring Stations. *Interagency Ecological Program Newsletter* 14(1):17–18.

Simenstad, C., J. Van Sickle, N. Monsen, E. Peebles, G. T. Ruggerone, and H. Gosnell. 2016. *Independent Review Panel Report for the 2016 California WaterFix Aquatic Science Peer Review*. Sacramento, CA: Delta Stewardship Council, Delta Science Program.

Thomson, J. R., W. J. Kimmerer, L. R. Brown, K. B. Newman, R. Mac Nally, W. A. Bennett, F. Feyrer, and E. Fleishman. 2010. Bayesian Change Point Analysis of Abundance Trends for Pelagic Fishes in the Upper San Francisco Estuary. *Ecological Applications* 20(5):1431–1448.

Vehtari, A., A. Gelman, and J. Gabry. 2017. Practical Bayesian model evaluation using leave-one-out cross-validation and WAIC. *Statistics and Computing* 27(5): 1413–1432.

Watanabe, S. 2010. Asymptotic equivalence of Bayes cross validation and widely applicable information criterion in singular learning theory. *Journal of Machine Learning Research* 11: 3571–3594.

Yao, Y., A. Vehtari, D. Simpson, and A. Gelman. 2018. Using Stacking to Average Bayesian Predictive Distributions (with Discussion). *Bayesian Analysis* 13(3):917–1007.

11F.8.2. Personal Communications

Nobriga, Matthew. Fish Biologist, Bay Delta Fish and Wildlife Office, U.S. Fish and Wildlife Service, Sacramento, CA. May 14, 2012—Email containing Excel file < logistic_parameters.xls> sent to Marin Greenwood, Aquatic Ecologist, ICF, Sacramento, CA.